Two-Component LDA Measurement in a Two-Phase Turbulent Jet

D. Modarress,* H. Tan,† and S. Elghobashi‡
Spectron Development Laboratories, Inc., Costa Mesa, California

The results of an experimental investigation of two-phase turbulent flow of air and solid particles in a round jet are presented. A method of laser Doppler anemometer (LDA) signal discrimination for two-phase flow measurement is proposed. It is shown that with a minimal modification of an existing two-component LDA system, the "cross talk" error caused by the signals from both phases can be eliminated. Data are presented in support of the effectiveness of this method. Extensive data for the two-phase turbulent round jet of air and 50-μm glass beads (mass loading ratio, $\phi_0 = 0.32$ and 0.85) are also presented. The measurements include profiles of mean velocity, turbulence intensity of both phases, and the gas-phase turbulent shear stress. The results indicate that the presence of the particles reduces the gas velocity fluctuations and the Reynolds shear stress. This reduction is proportional to the particle mass loading.

Introduction

THE necessity of studying two-phase flows arises in connection with several physical problems. Gas droplets and gas solid two-phase flows are common in aerosols, exhaust plumes, diesel engines, rocket nozzles, and pulverized coal combustors. As the mass loading ratio, defined as the mass flow rate of the dispersed phase to that of the continuous phase, is increased, the effect of the particles on the carrier fluid's turbulent transport of mass, momentum, and energy becomes more pronounced. This may strongly influence the overall efficiency of combustion.

The interaction between the two phases, in most practical flows, encompasses many phenomena which are not well understood at present. In order to delineate some of these complexities, there is a need to study them in a stepwise manner starting from simple well-defined flows. Here, we address the problem of modulation of the turbulent flowfield due to the presence of solid particles in a gaseous jet.

One of the earlier studies of turbulent two-phase jet flows was conducted by Laats,[1] who used dust particles ranging from 20 to 60 μm. He reported that centerline gas-phase velocity decay for two-phase flows was smaller than that for single-phase flows. Goldschmidt and Eskinazi[2] used hot wire to measure the local mean velocity and concentration of an aerosol in a two-phase turbulent plane jet. Hetsroni and Sokolov[3] investigated a round two-phase (oil droplets in air) turbulent jet. They employed hot-wire anemometry to obtain profiles of concentration, velocity, and intensity of turbulence. They observed that the presence of the dispersed phase reduces the intensity of turbulence, the spectral intensity, and the expansion rate of the turbulent jet. This reduction was found to increase with the concentration of the dispersed phase.

Popper et al.[4] used one component laser Doppler anemometer (LDA) to monitor the motion of 50-μm oil droplets in a round turbulent air jet. Their data showed the droplets' velocity decay along the jet axis to be slower than the axial velocity decay of the single-phase jet. They did not, however, report any gas-phase measurements. Recently, Girshovich et al.[5] reported the results of a comprehensive experimental investigation of spherical particles in air. Their data included mean velocity and the concentration profiles for a range of 35- to 67-μm particles and initial mass loadings of 0 to 1.5. No turbulence data were reported.

Modarress et al.[6] used a two-component laser anemometer and reported data for 50- and 200-μm particles in a turbulent two-phase axisymmetric jet. The data included mean gas and solid velocity profiles, particle concentration, as well as the profiles for the turbulence intensity and Reynolds shear stress.

The effects of the dispersed phase on the development of the jet as compared to a single-phase turbulent jet reported by the aforementioned authors are summarized as follows:

1) The expansion rate of a two-phase jet is smaller than that of a single-phase jet; this rate decreases as the initial mass loading is increased.

2) The centerline velocity decay of both phases in the turbulent jet is smaller than that of a single-phase turbulent jet.

3) The radial diffusion rate of the dispersed phase is smaller than that of the gas phase.

4) The mean slip velocity between the two phases increases with increasing particle diameter and decreases with increase in the initial mass loading.

5) The normalized velocity fluctuations are reduced with increase in the initial mass loading.

6) The normalized Reynolds shear stress for a two-phase turbulent jet is smaller than that of single-phase turbulent jet.

It is evident that in the past decade, some features of the two-phase turbulent jet with moderate mass loadings have been experimentally established and the data are, at least qualitatively, in general agreement. On the other hand, there are a number of unresolved issues for which there are either no published experimental data or the accuracy of the data is in question. One area of concern is the accuracy of the gas-phase velocity data in a two-phase flowfield. Hot-wire measurements are questionable at best. This is due to the nonlinear calibration requirement of the anemometer, as well as the possible contamination of the wire by the droplets present in the flow. Laser anemometry was successfully used by Durst and Zare[7] for measurement of the velocity of both phases in a two-phase flowfield. One main concern, however, has been the problem of "cross talk" between the signals obtained from the two phases. The ability to discriminate between the signals originating from the smaller particles which are assumed to closely follow the continuous phase and the signals originating from the larger particles or droplets

Presented as Paper 83-0052 at the AIAA 21st Aerospace Sciences Meeting, Reno, Nev., Jan. 10-13, 1983; submitted April 7, 1983; revision received July 21, 1983. This paper is declared a work of the U.S. Government and therefore is in the public domain.

*Senior Scientist. Member AIAA.

†Visiting Scientist, Institute of Mechanics, Chinese Academy of Science, Peking, China.

‡Associate Professor, Mechanical Engineering Department, University of California, Irvine, California. Member AIAA.

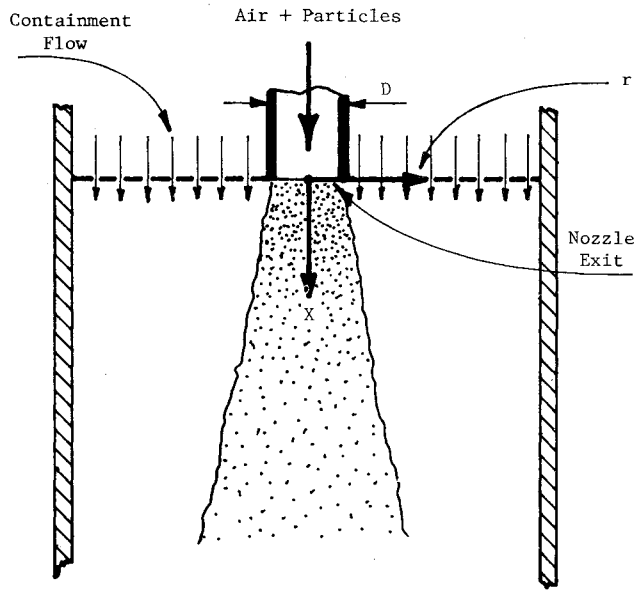

Fig. 1a Flowfield schematic.

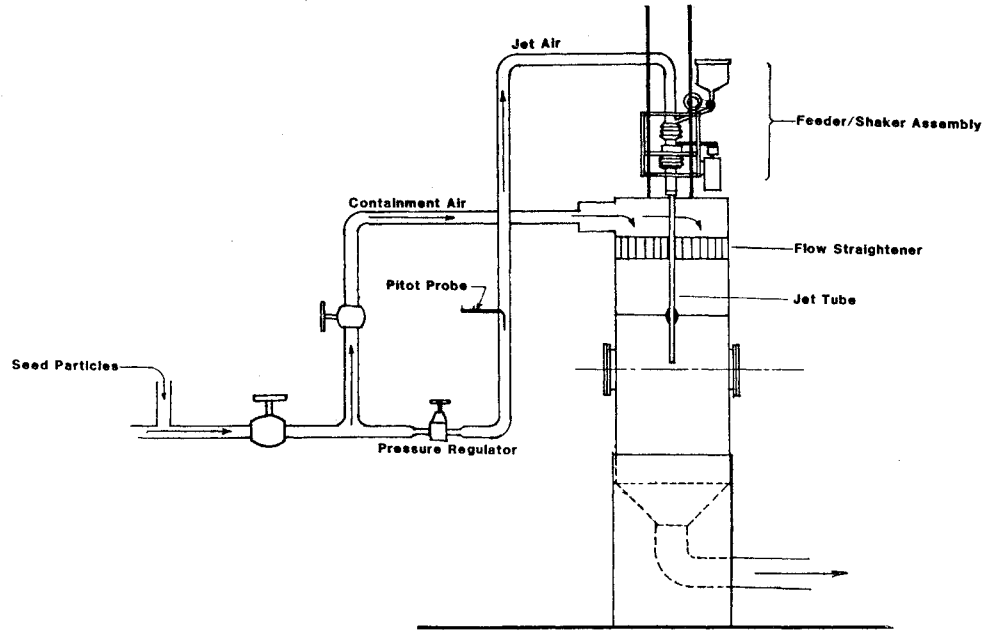

Fig. 1b Experimental setup.

(discrete phase) determines the accuracy of the data. The problem of cross talk becomes more severe as the mass loading ratio is increased.

The simplest form of a discriminator is an amplitude discriminator. This has been shown to be ineffective for high-particulate number densities. Lee and Durst[8] used a combination of amplitude discriminator and photo diodes resulting in a reduced cross talk between signals from the small and large particles.

The main purpose of this paper is to present a comprehensive set of data for an axisymmetric two-phase turbulent jet. Also presented is a novel method for signal discrimination which was developed during the course of this study in order to eliminate cross talk errors. Measurements are reported for components of mean velocities, turbulent intensities, and turbulent shear stress.

Experiment

Flowfield Configuration

The experimental configuration consisted of a 0.02-m-diameter pipe from which an air jet discharged into a low-velocity coflowing containment flow, Fig. 1. The diameter of the containment flow was 0.6 m. The pipe was 90 diameters long to provide a fully developed turbulent pipe flow at the exit.

Spherical glass beads of uniform size and material density of 2990 kg/m^3 were introduced into the jet from a hopper via a screw feeder. The solid mass flow rate was metered to within 2% of the nominal feed rate, as determined by the system calibration. The initial mass ratio ϕ_0, defined as the ratio of the total solid mass flow rate to the mass flow rate of the air at pipe exit, was changed from zero (single phase) to 0.85. Table 1 contains a complete list of the flow conditions at the pipe exit. A fixed height optical measurement station was provided with the capability of vertically moving the entire assembly of the feeder/shaker and jet tube in order to map the whole flowfield.

Laser Doppler Anemometer

The velocity measurements were made using a two-color, frequency shifted laser Doppler anemometer. Beam expansion capability was incorporated into both components. The collection angle was 30 deg off axis. A schematic of the

optics and the data management system (DMS) is given in Fig. 2. Single-particle, counter-type signal processing was used to measure the periods of the signal bursts produced by individual particles passing through the sensing volume. Micron-sized alumina tracer particles were injected at a constant rate into the main air supply. Care was taken to ensure a uniform seeding particle concentration across the jet boundaries. The data acquisition system had a coincidence check for the arrival time of bursts in each channel. This was done in order to ensure that both bursts originated from the same particle. Mean velocity, turbulence intensity, Reynolds shear stress, and higher order turbulent terms such as skewness and flatness were obtained.

At each location, the velocities of each phase were measured separately. By lowering the sensitivity of the LDA system to the smaller light-scattering seeding particles, only the light scattered from the larger dispersed phase was processed. For the gas-phase measurement in the presence of solid particles, the signals from the solid phase were identified and rejected. In general, the signal amplitude of the solid particles was larger than that of the seeding particles. For the case of small concentration flux of the solid phase, no direct discriminator for the solid/gas phase signals was needed. A combination of signal overload rejection and in some cases bandpass filtration was found to be sufficient to reject the signals from the solid phase. This method was used satisfactorily to discriminate against the signals from the 200-μm particles, $\phi_0 = 0.8$.

Table 1 Experimental flow conditions at $0.1D$ downstream of pipe exit

Gas-phase (air)	
Centerline velocity $U_{m,0}$, m/s	12.6
Exponent n of power-law velocity profile $U_g/U_{m,0} = [1-(2r/D)]\exp(1/n)$	6.6
Turbulence intensity $u'/U_{m,0} = 0.04 + 0.1\, r/D$	
Density ρ_g, kg/m^3	1.178
Mass flow rate $\dot{m}_g$, kg/s	3.76×10^{-3}
Reynolds number $R_e = 4\dot{m}_g/\pi\mu D$	13300
Uniform mean velocity of surrounding stream, m/s	0.05
Intensity of turbulence in surrounding stream	0.1
Solid-phase (glass beads)	
Particle diameter, μm	50
Particle density ρ_s, kg/m^3	2990
Centerline velocity $U_{s,0}$, m/s	12.4
Exponent n of power-law velocity profile	27.6
Case 1:	
Mass flow rate $\dot{m}_s$, kg/s	1.2×10^{-3}
Ratio of mass flow rates $\phi_0 = \dot{m}_s/\dot{m}_g$	0.32
Ratio of volumetric flow rates	1.1×10^{-4}
Case 2:	
Mass flow rate $\dot{m}_s$, kg/s	3.2×10^{-3}
Ratio of mass flow rate ϕ_0	0.85
Ratio of volumetric flow rates	2.9×10^{-4}

Auxiliary Pedestal Discriminator

Amplitude discriminators (AD) may detect large particles in the flow when they pass through the center portion of the probe volume. However, there is a finite probability that the large particles or droplets pass through the outside edge of the probe volume and, hence, the intensity of their signals may be below the AD's threshold. In this case, the signal is identified incorrectly. It can be shown[9] that for a typical LDA arrangement sensitive to the signal burst from a seeding particle (1 μm), with one decade window for the acceptable signal amplitude, 15% of the signals originating from the 50-μm particles will be incorrectly identified as those of the smaller seeding particles representing the gas phase. Number densities of 5000 and 10,000 per second have been assumed for the solid and gas phase, respectively. It can also be shown that for a constant solid mass ratio, the error is substantially increased as the particle size is decreased.

The auxiliary pedestal discriminator (APD) used in this study was designed to correctly identify the burst signal in one

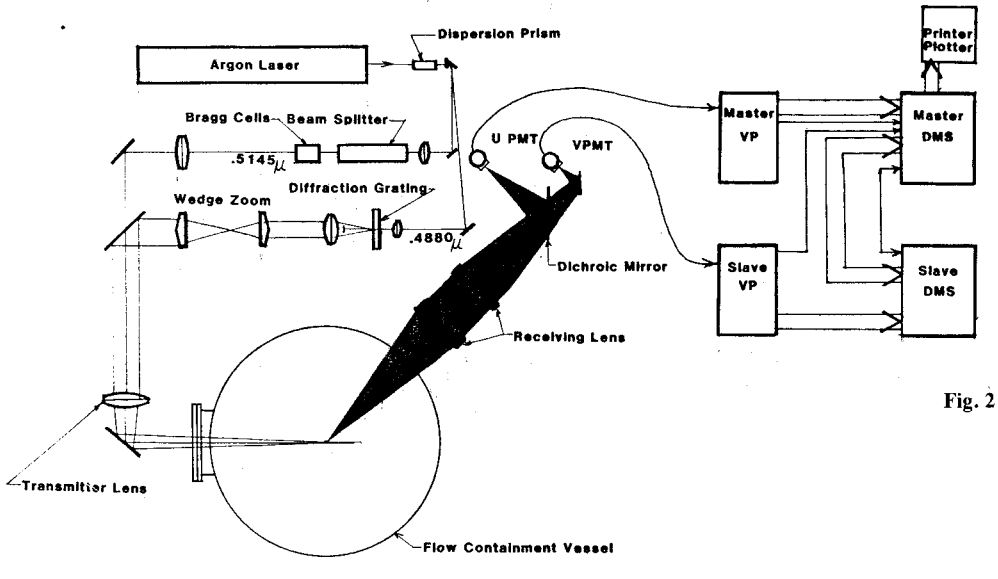

Fig. 2 Optics and data management system.

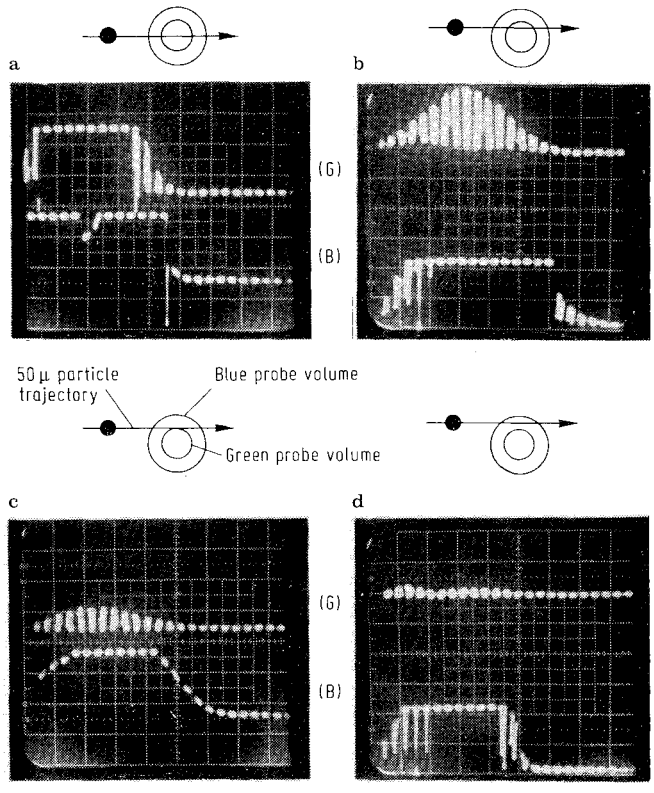

Fig. 3 Oscilloscope trace of signals from the green (G) and the blue (B) probes.

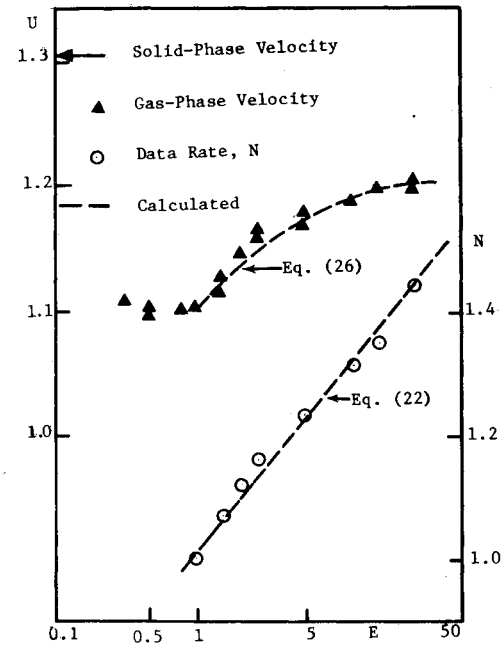

Fig. 4 Variation of the measured velocity U and data rate N with threshold voltage E.

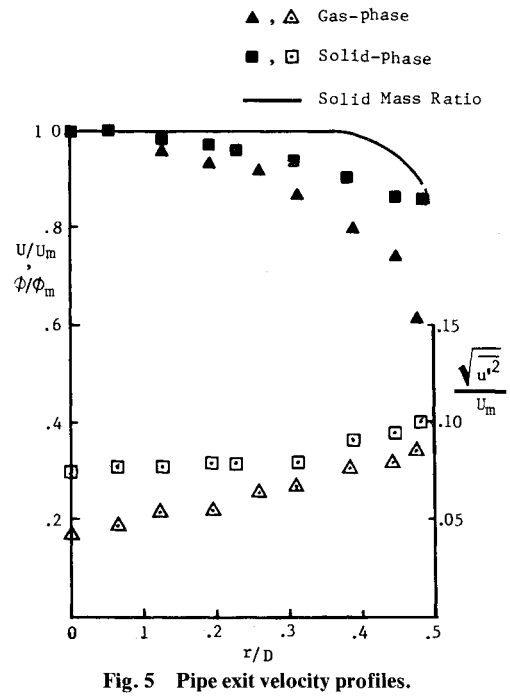

Fig. 5 Pipe exit velocity profiles.

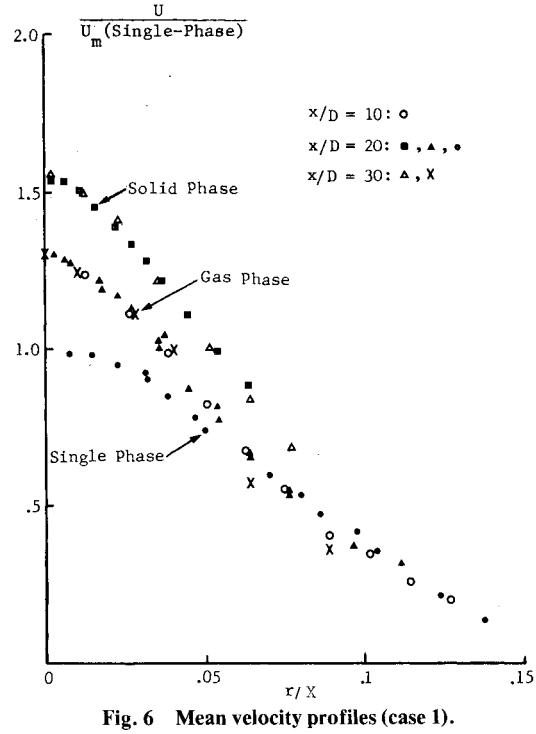

Fig. 6 Mean velocity profiles (case 1).

channel by monitoring the pedestal of the signal in the second channel. This was achieved by making the probe cross-sectional area of the second (auxiliary) channel larger than that of the first (primary) channel. The proper probe size for each color was determined based on the size of the solid particles. For the present flow, the probe volume of the green system (streamwise component) was set at about 100 μm ($1/e^2$ point) and that of the blue system was set at about 200 μm.

Figure 3 shows some typical oscilloscope traces of the signal bursts from the blue and green probes. The probable particle trajectories relative to the probe volumes are also included. The smaller circles depict the cross section of the green probe volume and the larger circles are those of the blue probe volume. In both cases, the signal from the blue channel will correctly identify the large particles. Hence, by monitoring the pedestal of the signal of the larger probe volume, the cross talk in the smaller probe volume may be eliminated. Because of the coincidence requirement of both signals, independent identification of the blue signal is not necessary.

The optimum setting of the variable threshold depends on the particle size and the optical parameters and must be experimentally determined. This optimization was carried out at $x/D=20$ and $r/x=0.03$. At that location the solid- and gas-phase velocities were separately measured by lowering the

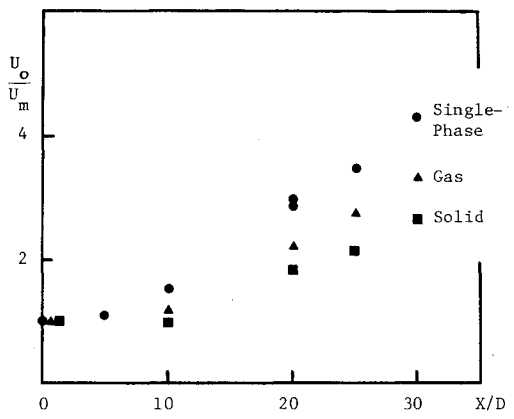

Fig. 7 Jet centerline mean velocity (case 1).

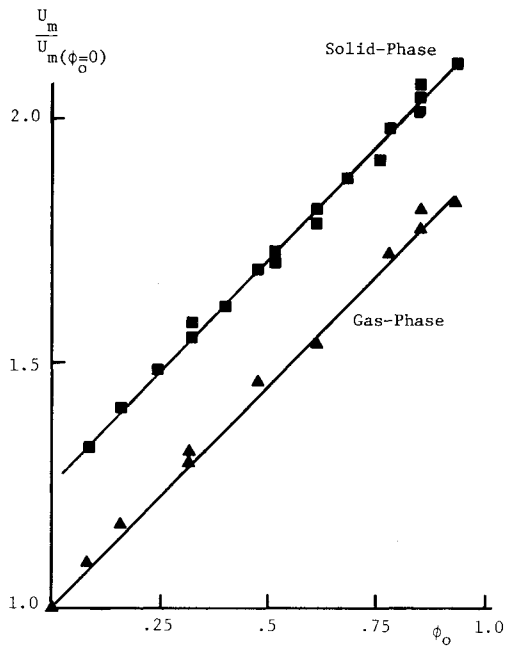

Fig. 8 Variation of axial mean velocity with initial solid mass loading, $x/D = 20$.

system power and setting the threshold voltage at its maximum. The solid-phase velocity, normalized by the single-phase velocity was 1.32. The gas-phase velocity, on the other hand, was measured for a number of threshold voltages and is given in Fig. 4. As the threshold voltage increased the data rate increased and the velocity, up to a critical point, remained constant (E = the voltage normalized to its value at this point). It is evident that for $E \leq 1$, the cross talk error is zero and that the measured velocity is the gas-phase velocity.

As E increased, the cross talk resulted in increased value for the mean velocity (solid triangles). This should be expected since the solid-phase velocity was 32% higher than that of the gas phase. Figure 4 also gives the plot of the data rate normalized to its value at $E = 1.0$. The data rate increased as the threshold level increased. Based on the assumption that the increased rate of the data acquisition reflected an increase in sampling of the solid phase, and using the values of the mean velocity of the two phases, the theoretical curve of U as a function of E was calculated and is shown in Fig. 4 as a dashed line. The agreement between the calculated and the measured values is good. Exponential increase in the data rate (linear on the log scale) as shown in the figure reflects the Gaussian distribution of the intensity of light in the sensing volume.

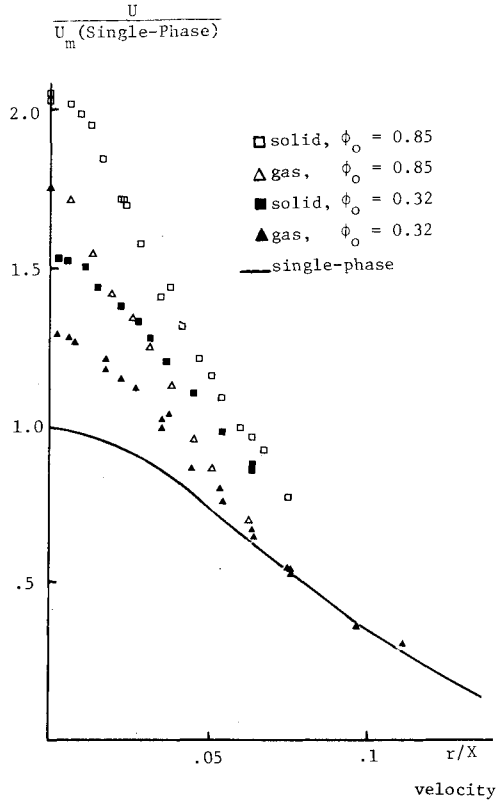

Fig. 9 Effect of mass loading on mean velocity profile, $x/D = 20$.

Results and Discussion

Results are presented for the mean velocity of the gas phase and the solid phase, velocity fluctuations of both phases, and the axial component of the Reynolds shear stress of the gas phase. Most of the data for 200-μm particles were reported in Ref. 6, while the data for the 50-μm solid particles will be discussed here.

At the pipe exit, the mean velocity and the turbulence intensity profiles for the solid phase (50 μm, $\phi_0 = 0.32$) are shown in Fig. 5. The gas-phase velocity profile agreed with a power-law distribution corresponding to a fully developed pipe flow (Table 1). The solid phase had a power-law velocity distribution. The solid-phase mass ratio across the exit is nearly uniform.

Mean Velocity

Velocity profiles of the single-phase and the two-phase (case 1) jets at axial locations $x/D = 10$, 20, and 30 are shown in Fig. 6. All the velocities are normalized with the single-phase mean centerline velocity at the corresponding axial location. The single-phase data agree well with those of Ref. 10. The gas-phase mean velocity is 30% higher than the single-phase velocity at the same position on the jet axis. In the outer portion of the jet the differences between the single-phase and the two-phase mean velocity were within the scatter of the data.

Variation of the mean velocity of single-phase and two-phase flows (case 1) along the jet centerline are given in Fig. 7. Single-phase results compare closely with the existing data (e.g., Ref. 10) with the virtual origin of the flow located 2 diameters downstream of the pipe exit. The presence of the solid phase inside the pipe had no measurable effect on the mean gas velocity at the pipe exit. This may be a feature of the test rig. The presence of the solid-phase, however, had a pronounced effect on the rate of decay of the mean velocity in the jet. Beyond the potential core region of the jet, the centerline gas-phase mean velocity was 30% higher than its value

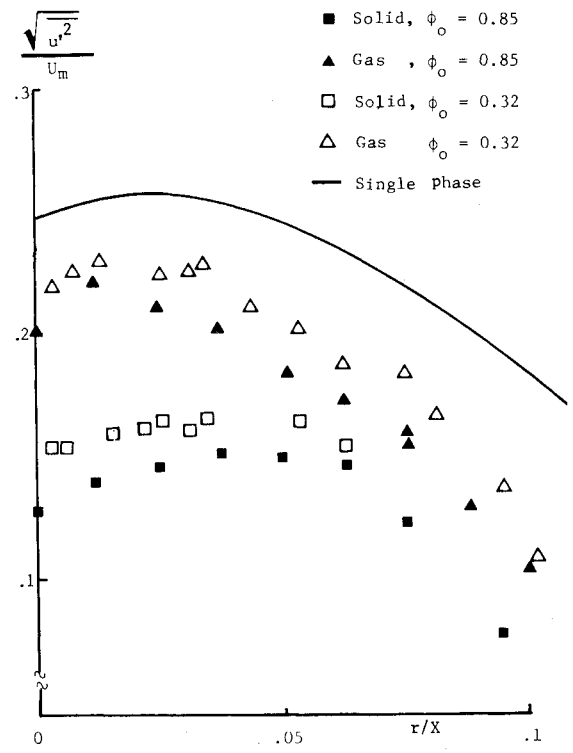

Fig. 10 Intensity of streamwise velocity fluctuation across the jet, $x/D = 20$.

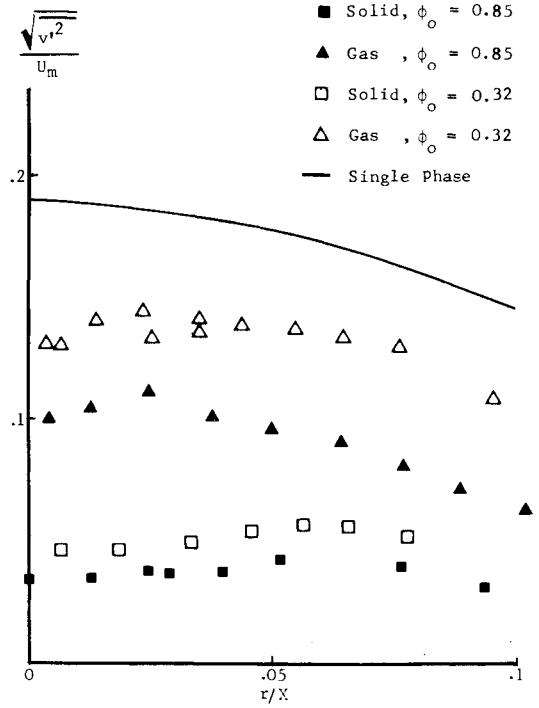

Fig. 11 Intensity of radial velocity fluctuation across the jet, $x/D = 20$.

for the single-phase flow and the mean slip velocity between the two phases remained close to 20% of the gas-phase mean axial velocity.

Effect of Solid-Phase Mass Loading

The present experimental data established that the gas-phase mean velocity at the pipe exit was independent of the mass loading ratio ϕ_0. The turbulence intensities, however, changed with ϕ_0. The effect of the mass loading on the mean

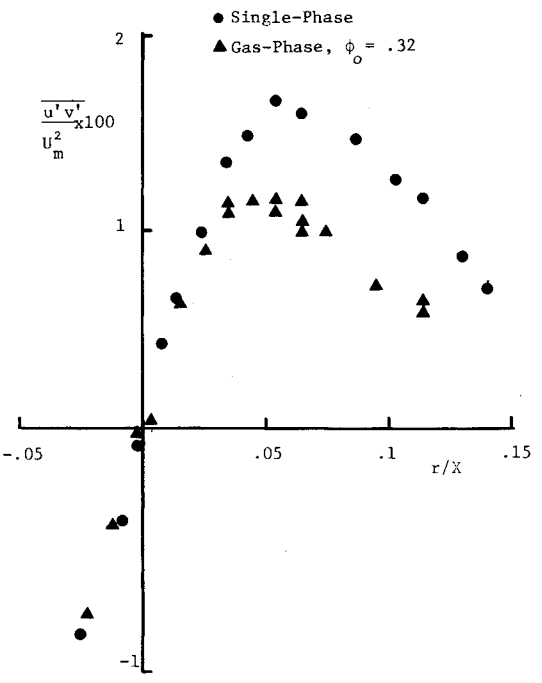

Fig. 12 Turbulent shear stress profiles, $x/D = 20$.

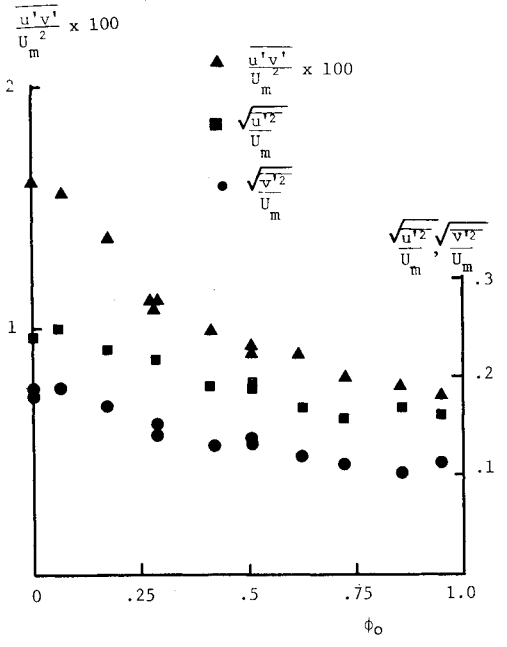

Fig. 13 Variation of turbulence intensities and maximum shear stress with ϕ_0.

velocities of the two phases was studied by measuring the centerline velocities at an axial position of $x/D = 20$. The variation of the mean velocities with ϕ_0 is shown in Fig. 8. The mean velocities, in the range of measurement, increased linearly with ϕ_0, whereas the absolute value of the mean slip velocity remained constant.

The effect of the initial mass loading ϕ_0 on the mean axial velocity profile is demonstrated in Fig. 9. Here, the gas and solid mean velocity profiles for $\phi_0 = 0.85$ (case 2) are compared with those for $\phi_0 = 0.32$ (case 1) taken from Fig. 6. The solid line shows the single-phase mean velocity profile. With increased solid mass loading, the mean velocities of both phases in the center region of the jet, where the local solid concentration is high, increase. This results in a narrower jet

for both phases. For $\phi_0 = 0.85$, the jet expansion rates for the solid and gas phases are 0.058 and 0.051, respectively. These values, when compared to the corresponding values of 0.07 and 0.064 for case 1, show a considerable reduction.

Also evident from Fig. 9 is that the mean slip velocity between the phases at each point, within the scatter of the data, is not a function of the local concentration flux of the particles. This observation is in support of the data of Fig. 8.

The effect of the solid-phase mass loading on the turbulence intensities was also investigated. Velocity fluctuations for both phases at the jet pipe exit were included in Fig. 5. The magnitude of the velocity fluctuation intensity across the pipe varied from 4% to 8% for the gas phase and to 9% for the solid phase. The corresponding values for the single-phase flow were 5 to 10%. Turbulence intensity profiles were also obtained at other axial locations and the data at $x/D = 20$ are shown in Figs. 10 and 11. The intensity (u'/U) profiles for single-phase and two-phase flows with $\phi_0 = 0.32$ and 0.85 are given in Fig. 10. The gas-phase turbulence intensities were generally lower than their single-phase values, but smaller changes were observed when mass loading was further increased. The solid-phase fluctuations were generally lower than those of the gas phase and the increase in the mass loading resulted in a slight decrease in the solid-phase velocity fluctuations.

The increase in the solid-phase mass loading had a more pronounced effect on the radial velocity fluctuations as given in Fig. 11. On the axis, the gas-phase radial fluctuations were reduced by 30% when compared with the single-phase values. Reduction of more than 50% in v' was measured for $\phi_0 = 0.85$ at $r/x \sim 0.1$. The solid-phase response to the radial fluctuation of the gas-phase flow was very slow resulting in a solid-phase radial velocity fluctuation of 4 to 6%. Increase in the mass loading had a measurable effect on the gas-phase velocity fluctuations and a smaller effect on the solid-phase fluctuations. Anisotropy of the turbulence at $x/D = 20$ was present in both the single- and two-phase flow.

The Reynolds shear stress $\overline{u'v'}$ was obtained by simultaneous sampling of the axial and radial velocities. The individual realizations of u_i and v_i were validated for coincidence and, consequently, their correlation coefficients were calculated. The profile of $\overline{u'v'}$ normalized with U_m^2 for the axial location of $x/D = 20$ is exhibited in Fig. 12. Here, the values of the gas-phase shear stress, when compared with those of the single-phase flow, show a reduction in the entire jet region, with the largest decrease sustained in the outer region of the jet. The maximum values for the shear stress for single- and two-phase flows were obtained at $r/x = 0.05$.

Variation of the maximum value of the Reynolds shear stress $\overline{u'v'}$ as a function of the initial mass loading is given in Fig. 13. The data were all obtained at $r/x = 0.05$. It shows a steep drop of shear stress up to $\phi_0 = 0.28$ and, eventually, more than 50% reduction when the mass loading is increased to 0.7.

Concluding Remarks

Two-phase flow of a round turbulent jet has been experimentally investigated. The cross talk error associated with the ambiguity of the LDA signal in two-phase flows has been discussed and a method of discrimination (APD) has been proposed. In the present study, incorporation of the discriminator into an existing LDA system was achieved through minor modifications of the optics and of the processor logic. The same concept could be applied to a one-component LDA system by use of either an auxiliary low-power laser of different wavelength or a third beam of different polarization.

Measurements included mean and fluctuating velocity components for each phase, as well as Reynolds shear stress for the gas phase. The flowfield conditions at the nozzle exit are provided in detail (Table 1) so as to allow critical evaluation of two-phase flow mathematical models.[11]

Normalized mean velocity profiles at axial locations $x/D = 10$, 20, and 30 show similarity within the accuracy of the measurement. This was true for both phases. The velocity profiles were otherwise shown to be a strong function of the mass loading. Increase in ϕ_0 resulted in narrower jets. The variation of the centerline mean velocities of both phases with the mass loading was also examined. Gas- and solid-phase mean velocities increased linearly with ϕ_0, up to $\phi_0 = 1$. The absolute value of the mean slip velocity remained constant.

Increasing the mass loading substantially reduced the radial velocity components of both phases. Smaller effect of the mass loading was observed for the streamwise velocity fluctuation. Finally, the effect of ϕ_0 on Reynolds shear stress was examined. Increasing ϕ_0 resulted in a reduction of the shear stress.

Acknowledgments

The work described herein was funded by the Department of Energy under Contract DE-F622-80PC-30303 to the University of California, Irvine.

References

[1] Laats, M. K., "Experimental Study of the Dynamics of an Air-Duct Jet," *Inzhenerno-Fizicheskii Zhurnal*, Vol. 10, Dec. 1966, pp. 11-15.

[2] Goldschmidt, V. and Eskinazi, S., "Two-Phase Turbulent Flow in a Plane Jet," *Journal of Applied Mechanics*, Vol. 33, Dec. 1966, pp. 735-747.

[3] Hetsroni, G. and Sokolov, M., "Distribution of Mass, Velocity, and Intensity of Turbulence in a Two-Phase Turbulent Jet," *Journal of Applied Mechanics*, Vol. 38, June 1971, pp. 315-327.

[4] Popper, J., Abuaf, N., and Hetsroni, G., "Velocity Measurements in a Two-Phase Turbulent Jet," *International Journal of Multiphase Flow*, Vol. 1, 1974, pp. 715-726.

[5] Girshovich, T. A., Kartushinskii, A. I., Laats, M. K., Leonov, V. A., and Mul'gi, A. S., "Experimental Investigation of a Turbulent Jet Carrying Heavy Particles of a Disperse Phase," *Izvestiya Akademii Nauk SSSR, Mekhanika Zhidkosti i Gaza*, No. 5, Sept.-Oct. 1981, pp. 26-31.

[6] Modarress, D., Wuerer, J., and Elghobashi, S., "An Experimental Study of a Turbulent Round Two-Phase Jet," AIAA Paper 82-0964, St. Louis, Mo., June 1982, to appear in *Chemical Engineering Communication*, 1984..

[7] Durst, F. and Zare, M., "Laser Doppler Measurement in Two-Phase Flows," *Proceedings of the LDA Symposium*, Copenhagen, Denmark, 1975, pp. 403-429.

[8] Lee, S. L. and Durst, F., "On the Motion of Particles in Turbulent Duct Flows," *International Journal of Multiphase Flow*, Vol. 8, No. 2, April 1982, pp. 125-146.

[9] Modarress, D. and Tan, H., "LDA Signal Discrimination in Two-Phase Flows," *Experiments in Fluids*, Vol. 1, Aug. 1983, pp. 1-6.

[10] Wygnanski, I. and Fiedler, H., "Some Measurements in the Self Preserving Jet," *Journal of Fluid Mechanics*, Vol. 38, Pt. 3, 1969, pp. 577-612.

[11] Elghobashi, S. E. and Abou-Arab, T. W., "A Two-Equation Turbulence Model for Two-Phase Flows," *Physics of Fluids*, Vol. 26, No. 4, April 1983, pp. 931-938.